Hindawi Publishing Corporation
Journal of Nanomaterials
Volume 2013, Article ID 101765, 6 pages
http://dx.doi.org/10.1155/2013/101765

Research Article

Thermal Annealing of Exfoliated Graphene

Wang Xueshen, Li Jinjin, Zhong Qing, Zhong Yuan, and Zhao Mengke

Division of Electricity and Quantum Metrology, National Institute of Metrology, Beijing 100013, China

Correspondence should be addressed to Wang Xueshen; wangxs@nim.ac.cn and Li Jinjin; jinjinli@nim.ac.cn

Received 20 February 2013; Revised 29 March 2013; Accepted 29 March 2013

Academic Editor: Raquel Verdejo

Monolayer graphene is obtained by mechanical exfoliation using scotch tapes. The effects of thermal annealing on the tape residues and edges of graphene are researched. Atomic force microscope images showed that almost all the residues could be removed in N_2/H_2 at 400°C but only agglomerated in vacuum. Raman spectra of the annealed graphene show both the 2D peak and G peak blueshift. The full width at half maximum (FWHM) of the 2D peak becomes larger and the intensity ratio of the 2D peak to G peak decreases. The edges of graphene are completely attached to the surface of the substrate after annealing.

1. Introduction

Isolated graphene was first prepared by mechanical exfoliation of highly oriented pyrolytic graphite (HOPG) [1]. Such exfoliated graphene exhibits high crystal quality and draws significant attention because of its unique electrical properties [2–5]. The mobility of the exfoliated graphene could be as high as 200000 $cm^2 \cdot V^{-1} \cdot s^{-1}$ [6, 7] which allows for the observation of quantum Hall effect even at room temperature [8]. Therefore it is a promising candidate for a high-temperature quantum resistance standard [9–13] for metrology applications.

The graphene films, obtained by micromechanical exfoliation [1, 14, 15], synthesized from chemical vapor deposition [16–18] and epitaxial methods [19, 20], usually suffer from the surface contaminations which affect their intrinsic electrical properties. Currently many methods are being investigated for removing the surface resist residues of the graphene films introduced by transfer and E-beam lithography process. Among these methods, thermal annealing is shown to be very reproducible [21–23]. However, insufficient attention has been paid to the surface cleaning issue of the exfoliated graphene films before device fabrication [24]. The scotch tape residues on the exfoliated graphene films need to be removed in order to fabricate high-quality devices.

In this paper, we demonstrate the effect of thermal annealing for removing the tape residues of the exfoliated graphene films and flattening the edges. The thermal annealing process is optimized by adjusting the annealing gases and the temperature. AFM and Raman spectroscopy are used to characterize the annealed films.

2. Materials and Methods

Graphene films are obtained by mechanical exfoliation of Kish graphite with 3 M magic scotch tapes and then transferred to the SiO_2 (300 nm)/Si substrate. Optical microscope is first used to locate the graphene. Raman spectra measurements are then performed on a LabRAM HR800 with the wavelength of 632.8 nm to identify the layer number of the graphene. Atomic force microscope (AFM) is used to characterize the surface of graphene with the tapping mode and an insulating probe.

Two pieces of graphene are achieved on the SiO_2 substrate in one exfoliation process referred to as M1 and M2, respectively, for contrast experiments. Acetone is first used to clean the films. Optical images of the researched graphene are shown in Figure 1(a) for M1 and Figure 1(b) for M2, respectively. We can observe that there are still tape residues on and beside the graphene M1 and M2 indicated by white circles even after cleaning with acetone. These residues will increase the contact resistance and affect the attachment of electrode metals, thus should be removed before device fabrication.

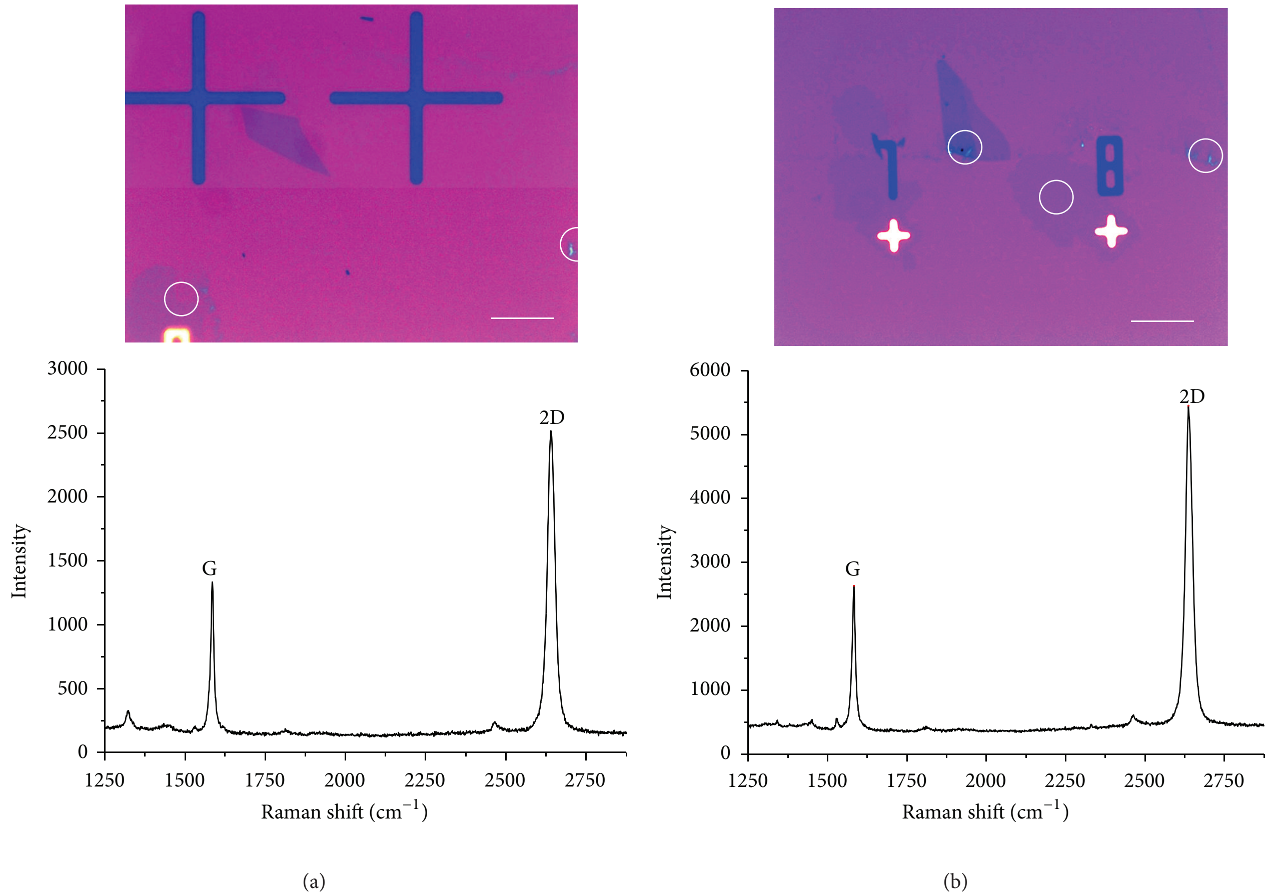

FIGURE 1: Optical images (top) and the corresponding Raman spectra (bottom) of monolayer graphene M1 (a) and M2 (b) on SiO_2/Si before annealing. The scale bars are 10 μm in length (colors online).

The FWHM of 2D peak is the key factor to determine the number of layers of graphene which is lower than 40 cm^{-1} with a single Lorenz peak for monolayer graphene. The FWHMs of the 2D peaks of M1 and M2 are both 24 cm^{-1}, and they are highly symmetrical and also can be fitted with a single Lorenz peak [25]. Therefore, the researched samples M1 and M2 are both monolayer graphene.

Thermal annealing is performed using an annealing oven with N_2/H_2 and low pressure of 5 mbar. The heating and cooling rate should be low to prevent the edge of the graphene from folding or rolling up [26]. In our studies, both heating and cooling rates are 6°C/min. The annealing conditions of samples M1 and M2 are shown in Table 1. Graphene M1 is first annealed at 300°C and then 400°C subsequently in vacuum at a pressure of 5 mbar and lastly annealed at 400°C in N_2/H_2 at a flow rate of 200 cm^3/min (sccm) and 50 sccm and a pressure of 50 mbar for 2 hours. For M2, annealing at 300°C and 400°C subsequently in N_2/H_2 at a pressure of 50 mbar for 2 hours is performed.

TABLE 1: Annealing conditions of monolayer graphene M1 and M2.

Annealing no.	Sample	
	M1	M2
1	300°C, 5 mbar, 2 hours	300°C, 50mbar, 2 hours N_2/H_2 (200 sccm/50 sccm)
2	400°C, 5 mbar, 2 hours	400°C, 50 mbar, 2 hours N_2/H_2 (200 sccm/50 sccm)
3	400°C, 50 mbar, 2 hours N_2/H_2 (200 sccm/50 sccm)	

3. Results and Discussion

Figure 2 shows the AFM topographic images and the Raman spectra of M1 before and after each annealing step. Before annealing, the tape residues form films on and beside M1 as shown in the AFM image of Figure 2(a). The Raman peaks between 1100 cm^{-1} and the G peak are due to the tape residue films. After annealing at 300°C in vacuum for 2 h, the residue film on the surface of M1 agglomerates to large particles and that beside M1 becomes thinner as shown in the AFM image of Figure 2(b). The peaks of the tape residues

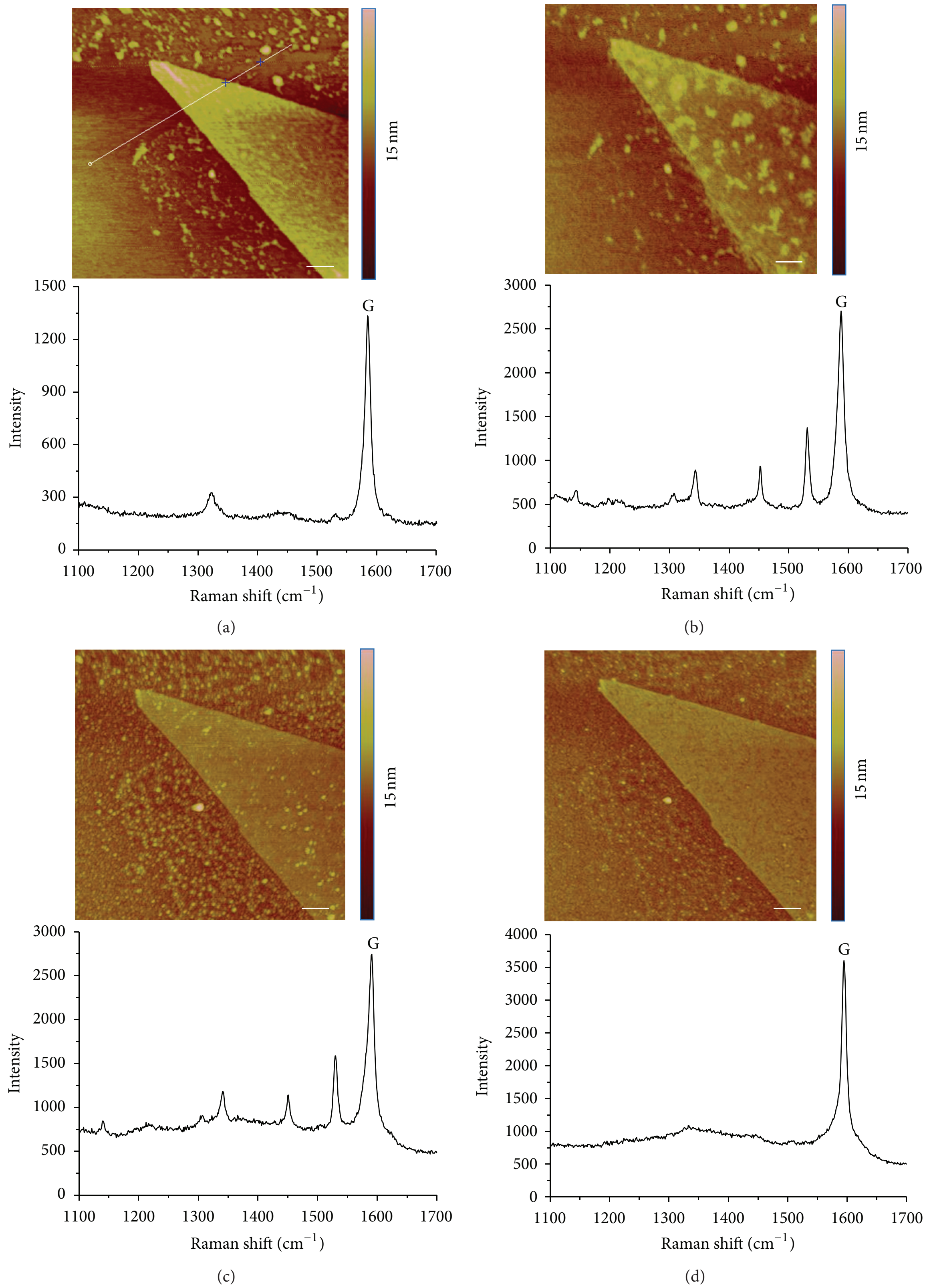

FIGURE 2: AFM topographic images (top) and the corresponding Raman spectra (bottom) of graphene M1. (a) Before annealing; (b) annealing at 300°C in vacuum of 5 mbar; (c) annealing at 400°C in vacuum of 5 mbar; (d) annealing at 400°C in N_2/H_2 of 50 mbar. Scale bars are 300 nm in length (colors online).

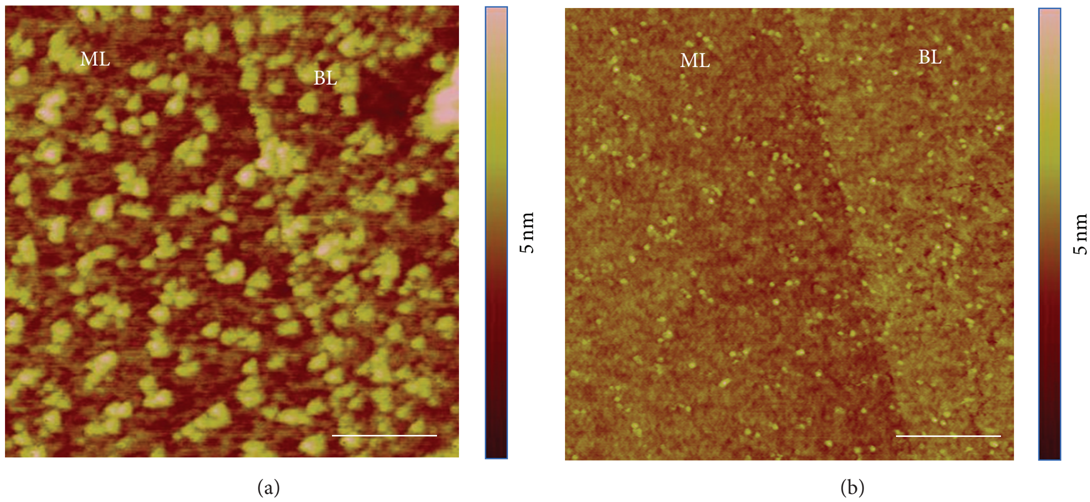

Figure 3: AFM topographic images of the graphene M2 after annealing in N_2/H_2 at 300°C (a) and 400°C (b); left part of the graphene M2 is monolayer (ML) and the right part is bilayer (BL). Scale bars are 300 nm in length (colors online).

are still present in the corresponding Raman spectrum and the intensity ratios of these peaks to the G peak become larger which indicates that the residues are not removed. D peak at 1340 cm^{-1} also emerges. Annealing temperature is raised to 400°C in vacuum for 2 h, the surface residue particles diminish, and those on the substrate become much smaller ones that are distributed more evenly as illustrated in Figure 2(c). The Raman spectrum clearly shows that the residues are not completely removed although the intensity ratios decrease.

It is obvious that annealing in vacuum does not efficiently remove the tape residues on the surface of the graphene. The residues just congregate to particles from films and change the positions continuously. N_2/H_2 gas is introduced into the oven for further annealing the graphene M1 at rates of 200 sccm and 50 sccm, respectively, and the pressure is 50 mbar. The annealing result is shown in Figure 2(d). The AFM image shows that the surface is much smoother than that in Figure 2(b). Most of the surface area of M1 is now close to the substrate, indicating that the surface shows similar roughness with the substrate. The absence of the intrinsic tape residue peaks in the corresponding spectrum confirms the nearly complete removal of the residues on the surface of the monolayer graphene M1.

We can also observe that the edge of M1 does not contact fully with the substrate surface in Figure 2(a). This kind of disengagement from the surface of SiO_2 may cause graphene's rolling up from the edge. The height values between the two blue forks on the white line marked on the graphene M1 in Figure 2(a) are measured before annealing, after 300°C annealing in vacuum, after 400°C annealing in vacuum, and after 400°C annealing in N_2/H_2 to be 3.1 nm, 1.9 nm, 1.6 nm, and 1.2 nm. The height of the edge of M1 decreases accompanying annealing and 1.2 nm is already at the level of the thickness of a graphene film on the surface of SiO_2 [1, 27]. Therefore, the edge of M1 becomes fully attached to the substrate.

Compared with the characterization results of annealing in vacuum and N_2/H_2, it is concluded that N_2/H_2 gas is essential in removing the tape residues on the surface of graphene. The mechanism of this gas effect on the removing tape residues is still on research. We speculate that the removal of tape residues on the surface of graphene may be due to the reaggregation of the tape residues and the chemical decomposition of the residues. The introduction of N_2/H_2 may help the gasification of scission products. Successive researches on the mechanism of N_2/H_2 helping for removing tape residues are in progress.

The effect of the annealing temperature of N_2/H_2 gas is also studied on the monolayer graphene M2. The topographic AFM images of M2 after annealing are shown in Figure 3. There are still few tape residue particles on the surface of M2 after annealing in N_2/H_2 at 300°C as shown in Figure 3(a). However, these particles nearly vanish after further annealing at 400°C confirmed by the AFM image shown in Figure 3(b). This indicates that high temperature is advantageous for the removing of the tape residues.

G and 2D peaks in the Raman spectrum are used to characterize the effect of annealing on the graphene M1 and M2. The blueshifts of the G peak of M1 and M2 are 10 cm^{-1} and 11 cm^{-1} and the 2D peaks blue-shifts are 12 cm^{-1} and 11 cm^{-1}, respectively, as shown in Figures 4(a) and 4(b), respectively. It is known that the blue-shift can be caused by either strain [28, 29] or hole doping [23, 24, 30–33]. In our case, the blueshifts of the G peak and 2D peak are close, which implies that hole doping is the main cause of the blue-shift since the 2D peak is more sensitive to strain than the G peak. For the graphene M1, the FWHM of the 2D peak increases with annealing temperatures both in vacuum and N_2/H_2, as shown in Figure 4(c). This is due to the increase of the disorders which affect the formation of the 2D peak and the strengthening of the interreaction between M1 and the SiO_2 substrate with progressive annealing [34]. However, the FWHM of the 2D peak for M2 changes significantly after

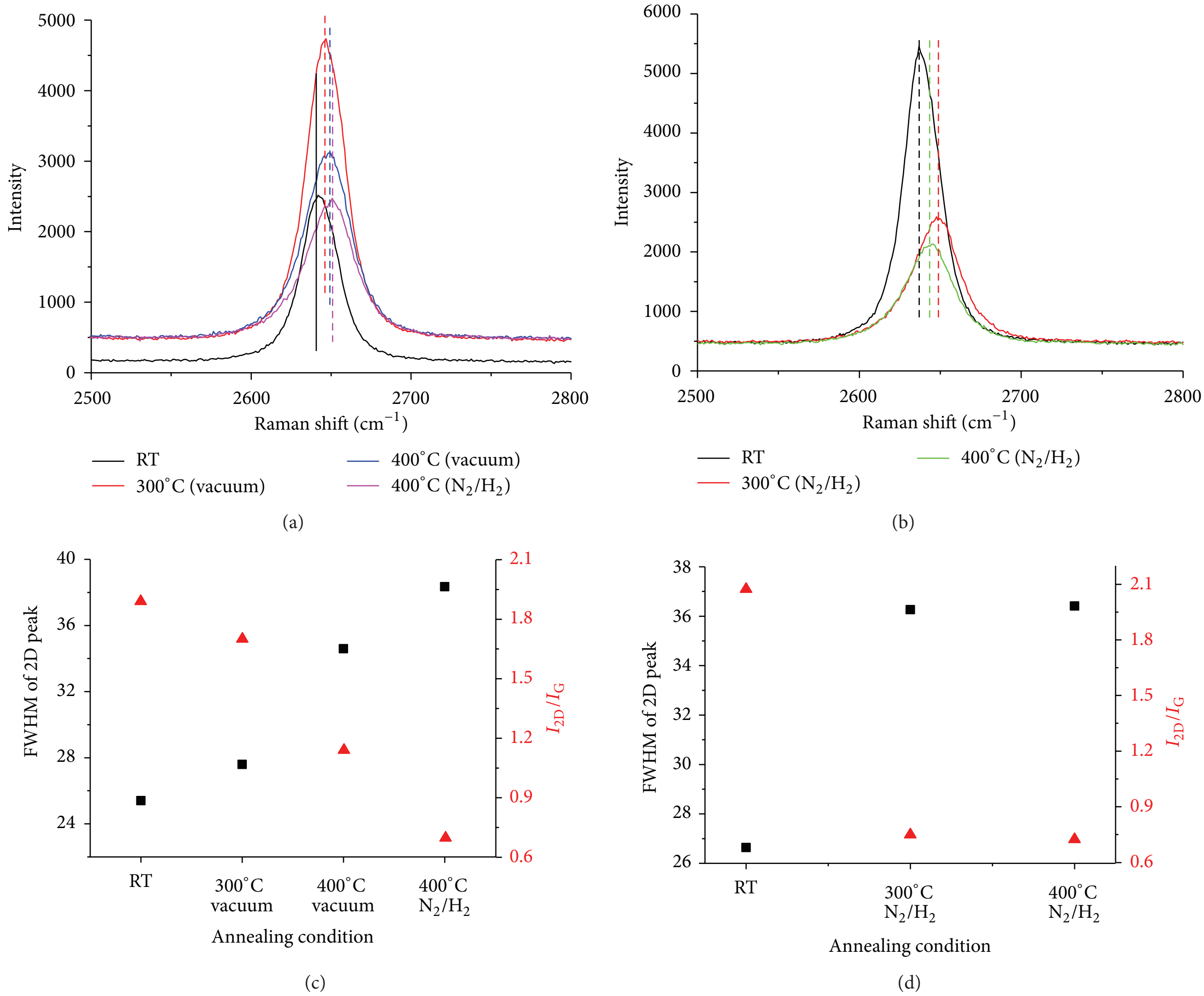

FIGURE 4: The 2D peaks of graphene M1 (a) and M2 (b) after each annealing step; the FWHM (black) of 2D peak and the intensity ratio (red) of the 2D peak and G peak for graphene M1 (c) and M2 (d) (colors online).

annealing at 300°C but increments marginally after the following annealing at 400°C in N_2/H_2 as shown in Figure 4(d). It can be concluded that the disorders emerge in the removing and moving processes of the tape residues. Most of the tape residues are removed by annealing at 300°C in N_2/H_2 that left few residues being removed in the annealing process at 400°C in N_2/H_2. Thus the broadening of the 2D peak of M2 is different for the two steps. The intensity ratio of I_{2D}/I_G which is sensitive to doping [34, 35] decreases with the increasing annealing temperature for both graphene M1 and M2 as shown in Figures 4(c) and 4(d) by the red axes.

4. Conclusions

In conclusion, monolayer graphene is prepared using scotch tape to mechanically exfoliate Kish graphite and thermal annealing in vacuum or N_2/H_2 is performed to remove the tape residues left on the surface of and beside graphene. The annealing effect is characterized by AFM and Raman spectra from which we confirm that annealing in vacuum is not effective to remove the tape residues and N_2/H_2 is critical. Also increasing the temperature is helpful for residue removal. Tape residues can be removed by annealing at 400°C in N_2/H_2 at a pressure of 50 mbar for 2 h. Thermal annealing brings hole doping in graphene which accounts for the blueshifts of the G peak and the 2D peak and the decrease of the I_{2D}/I_G intensity ratio in Raman spectra. The 2D peaks broaden due to the emerging disorders during the annealing process and the enhanced interreaction between graphene and SiO_2 substrate. The edges of graphene completely attach the surface of the substrates after thermal annealing processes.

Acknowledgment

This work was supported by the National Key Technology R&D Program (20-1125ZCKF).

References

[1] K. S. Novoselov, A. K. Geim, S. V. Morozov et al., "Electric field in atomically thin carbon films," *Science*, vol. 306, no. 5696, pp. 666–669, 2004.

[2] A. K. Geim and K. S. Novoselov, "The rise of graphene," *Nature Materials*, vol. 6, no. 3, pp. 183–191, 2007.

[3] A. H. C. Neto, F. Guinea, N. M. R. Peres, K. S. Novoselov, and A. K. Geim, "The electronic properties of graphene," *Reviews of Modern Physics*, vol. 81, no. 1, pp. 109–162, 2009.

[4] T. Ihn, J. Güttinger, F. Molitor et al., "Graphene single-electron transistors," *Materials Today*, vol. 13, no. 3, pp. 44–50, 2010.

[5] A. S. Mayorov, R. V. Gorbachev, S. V. Morozov et al., "Micrometer-scale ballistic transport in encapsulated graphene at room temperature," *Nano Letters*, vol. 11, no. 6, pp. 2396–2399, 2011.

[6] K. I. Bolotin, K. J. Sikes, Z. Jiang et al., "Ultrahigh electron mobility in suspended graphene," *Solid State Communications*, vol. 146, no. 9-10, pp. 351–355, 2008.

[7] S. V. Morozov, K. S. Novoselov, M. I. Katsnelson et al., "Giant intrinsic carrier mobilities in graphene and its bilayer," *Physical Review Letters*, vol. 100, no. 1, Article ID 016602, 4 pages, 2008.

[8] K. S. Novoselov, Z. Jiang, Y. Zhang et al., "Room-temperature quantum hall effect in graphene," *Science*, vol. 315, no. 5817, p. 1379, 2007.

[9] Y. Zhang, Y. W. Tan, H. L. Stormer, and P. Kim, "Experimental observation of the quantum Hall effect and Berry's phase in graphene," *Nature*, vol. 438, no. 7065, pp. 201–204, 2005.

[10] K. S. Novoselov, A. K. Geim, S. V. Morozov et al., "Two-dimensional gas of massless Dirac fermions in graphene," *Nature*, vol. 438, no. 7065, pp. 197–200, 2005.

[11] A. J. M. Giesbers, G. Rietveld, E. Houtzager et al., "Quantum resistance metrology in graphene," *Applied Physics Letters*, vol. 93, no. 22, Article ID 222109, 2008.

[12] S. Tanabe, Y. Sekine, H. Kageshima, M. Nagasey, and H. Hibino, "Half-integer quantum hall effect in gate-controlled epitaxial graphene devices," *Applied Physics Express*, vol. 3, no. 7, Article ID 075102, 3 pages, 2010.

[13] A. Tzalenchuk, S. Lara-Avila, A. Kalaboukhov et al., "Towards a quantum resistance standard based on epitaxial graphene," *Nature Nanotechnology*, vol. 5, no. 3, pp. 186–189, 2010.

[14] A. Reina, H. Son, L. Jiao et al., "Transferring and identification of single- and few-layer graphene on arbitrary substrates," *Journal of Physical Chemistry C*, vol. 112, no. 46, pp. 17741–17744, 2008.

[15] M. H. Gass, U. Bangert, A. L. Bleloch, P. Wang, R. R. Nair, and A. K. Geim, "Free-standing graphene at atomic resolution," *Nature Nanotechnology*, vol. 3, no. 11, pp. 676–681, 2008.

[16] X. Li, W. Cai, J. An et al., "Large-area synthesis of high-quality and uniform graphene films on copper foils," *Science*, vol. 324, no. 5932, pp. 1312–1314, 2009.

[17] K. S. Kim, Y. Zhao, H. Jang et al., "Large-scale pattern growth of graphene films for stretchable transparent electrodes," *Nature*, vol. 457, no. 7230, pp. 706–710, 2009.

[18] Y. Yamazaki, M. Wada, M. Kitamura et al., "Low-Temperature graphene growth originating at crystalline facets of catalytic metal," *Applied Physics Express*, vol. 5, no. 5, Article ID 025101, 3 pages, 2012.

[19] P. N. First, W. A. De Heer, T. Seyller, C. Berger, J. A. Stroscio, and J. S. Moon, "Epitaxial graphenes on silicon carbide," *MRS Bulletin*, vol. 35, no. 4, pp. 296–305, 2010.

[20] L. Huang, W. Y. Xu, Y. D. Que et al., "The influence of annealing temperature on the morphology of graphene islands," *Chinese Physics B*, vol. 20, no. 8, Article ID 088102, 2012.

[21] A. Pirkle, J. Chan, A. Venugopal et al., "The effect of chemical residues on the physical and electrical properties of chemical vapor deposited graphene transferred to SiO_2," *Applied Physics Letters*, vol. 99, no. 12, Article ID 122108, 3 pages, 2011.

[22] Y. C. Lin, C. C. Lu, C. H. Yeh, C. H. Jin, K. Suenaga, and P. W. Chiu, "Graphene annealing: how clean can it be?" *Nano Letters*, vol. 12, no. 1, pp. 414–419, 2012.

[23] Z. Cheng, Q. Zhou, C. Wang, Q. Li, C. Wang, and Y. Fang, "Toward intrinsic graphene surfaces: a systematic study on thermal annealing and wet-chemical treatment of SiO_2-supported graphene devices," *Nano Letters*, vol. 11, no. 2, pp. 767–771, 2011.

[24] Z. H. Ni, H. M. Wang, Z. Q. Luo et al., "The effect of vacuum annealing on graphene," *Journal of Raman Spectroscopy*, vol. 41, no. 5, pp. 479–483, 2010.

[25] A. C. Ferrari, J. C. Meyer, V. Scardaci et al., "Raman spectrum of graphene and graphene layers," *Physical Review Letters*, vol. 97, no. 18, Article ID 187401, 4 pages, 2006.

[26] N. H. Su, M. Liu, and F. Liu, "Chemical versus thermal folding of graphene edges," *Nano Research*, vol. 4, no. 12, pp. 1242–1247, 2011.

[27] X. Li, X. Wang, L. Zhang, S. Lee, and H. Dai, "Chemically derived, ultrasmooth graphene nanoribbon semiconductors," *Science*, vol. 319, no. 5867, pp. 1229–1232, 2008.

[28] Z. H. Ni, T. Yu, Y. H. Lu, Y. Y. Wang, Y. P. Feng, and Z. X. Shen, "Uniaxial strain on graphene: Raman spectroscopy study and band-gap opening," *ACS Nano*, vol. 2, no. 11, pp. 2301–2305, 2008.

[29] T. M. G. Mohiuddin, A. Lombardo, R. R. Nair et al., "Uniaxial strain in graphene by Raman spectroscopy: G peak splitting, Grüneisen parameters, and sample orientation," *Physical Review B*, vol. 79, no. 20, Article ID 205433, 8 pages, 2009.

[30] A. Das, S. Pisana, B. Chakraborty et al., "Monitoring dopants by Raman scattering in an electrochemically top-gated graphene transistor," *Nature Nanotechnology*, vol. 3, no. 4, pp. 210–215, 2008.

[31] L. M. Malard, M. A. Pimenta, G. Dresselhaus, and M. S. Dresselhaus, "Raman spectroscopy in graphene," *Physics Reports*, vol. 473, no. 5-6, pp. 51–87, 2009.

[32] L. M. Malard, R. L. Moreira, D. C. Elias, F. Plentz, E. S. Alves, and M. Pimenta, "Thermal enhancement of chemical doping in graphene: a Raman spectroscopy study," *Journal of Physics Condensed Matter*, vol. 22, no. 33, Article ID 334202, 2010.

[33] A. Nourbakhsh, M. Cantoro, A. Klekachev et al., "Tuning the fermi level of SiO_2-supported single-layer graphene by thermal annealing," *Journal of Physical Chemistry C*, vol. 114, no. 15, pp. 6894–6900, 2010.

[34] B. Tang, G. Hu, and H. Y. Gao, "Raman spectroscopic characterization of graphene," *Applied Spectroscopy Reviews*, vol. 45, no. 5, pp. 369–407, 2010.

[35] Z. H. Ni, H. M. Wang, Y. Ma, J. Kasim, Y. H. Wu, and Z. X. Shen, "Tunable stress and controlled thickness modification in graphene by annealing," *ACS Nano*, vol. 2, no. 5, pp. 1033–1039, 2008.